Synthesis and Characterization of Mononuclear and Dinuclear Ruthenium Complexes with Tris(2-pyridylmethyl)amine and Tris(5-methyl-2-pyridylmethyl)amine

Takahiko Kojima,*,† Takayuki Amano,† Youichi Ishii,‡ Masaaki Ohba,† Yoshihiro Okaue,† and Yoshihisa Matsuda*,†

Department of Chemistry, Faculty of Science, Kyushu University, Hakozaki, Higashi-Ku, Fukuoka 812-81, Japan, and Department of Chemistry and Biotechnology, The Graduate School of Engineering, The University of Tokyo, Hongo, Bunkyo-Ku, Tokyo 113, Japan

Received August 19, 1997

Novel Ru(II) and Ru(III) complexes having TPA (tris(2-pyridylmethyl)amine, L1) and 5-Me_3-TPA (tris(5-methyl-2-pyridylmethyl)amine, L2) were prepared to establish their synthetic routes and to elucidate coordination geometry and interactions between tightly bound tripodal tetradentate ligands and Ru^{II}/Ru^{III} centers. They include mononuclear Ru(II) complexes $[RuCl(DMSO)(L)]ClO_4$ (**1** (L1), **2** (L2)), dinuclear bis-μ-chloro Ru(II) complexes $[RuCl(L)]_2(ClO_4)_2$ (**3** (L1), **4** (L2)), and mononuclear Ru(III) complexes $[RuCl_2(L)]ClO_4$ (**5** (L1), **6** (L2)). They were characterized by X-ray crystallography (for **2**, **3**, and **5**), ^1H NMR spectroscopy, and cyclic voltammetry. For compound **2**, the crystal structure was determined to possess S-bound DMSO ligand which was trans to pyridine and Cl^- trans to the tertiary amino group of L2, and this isomer was obtained exclusively. Complex **1** was also isolated as a single isomer. Complex **3** was revealed to be a dinuclear bis-μ-chloro Ru(II) species with the center of symmetry midway between two Cl^-. ^1H NMR spectra of Ru(II) complexes **1**−**4**, the molecular structure of **2**, and comparison of the molecular structure of **3** with **5** suggest that the interaction between the Ru(II) center, pyridyl moieties, and the DMSO ligand is strengthened by π-back-bonding from the Ru(II) center to the ligands in addition to σ-bonding of the tertiary amino group. Electrochemical measurements on **1**−**6** in CH_3CN revealed that the methyl groups on pyridyl rings exert electron-donating effects onto the Ru centers to lower each redox process and such effect strengthens the Ru−S bonding in **2** compared with that in **1**, accommodating π-back-bonding from Ru(II) center to other π-acceptors such as DMSO in **2** enough to prevent isomerization of DMSO binding mode. The dinuclear complexes **3** and **4** showed relatively large comproportionation constants, which suggest mixed-valent $Ru^{II}Ru^{III}$ states would be stabilized.

Introduction

TPA (tris(2-pyridylmethyl)amine) and its derivatives have made significant contributions to understanding of metalloenzymes through their structural and functional modeling for dinuclear and mononuclear active sites which contain Fe,Cu sites as dioxygen activation centers.[1,2] Therefore, their versatility will engender some new aspects of other transition metal chemistry in terms of physical properties and chemical reactivity at the metal center.

Other than the first-row transition metals, few second- and third-row transition metals have been the target of exploration of chemical properties by using TPA and its derivatives. Recently, Sasaki and co-workers devoted their synthetic efforts on Re complexes involving bis(μ-oxo) dinuclear complexes[3] and high-valent Re═O species with TPA in a tetradentate form and a tridentate fashion which possesses one uncoordinated pyridylmethyl arm.[4]

We have focused on the character of TPA: The TPA ligands include three π-acceptors (pyridyl group) and one σ-donor (tertiary amino group) and could provide thermodynamic stability of complexes formed by its tetradentate chelation. It has been a central issue to elucidate π-back-bonding interactions from Ru center to pyridine derivatives, so that such interactions play indispensable roles in the light of a variety of interesting excited-states behaviors involving photoredox reactions, luminescence, photosubstitution, and photoinduced electron transfer.[5−9]

* To whom correspondence should be addressed. Fax: +81 92 642 2570. E-mail: cosyscc@mbox.nc.kyushu-u.ac.jp (T.K.) and matsuscc@mbox.nc.kyushu-u.ac.jp (Y.M.).

† Kyushu University.

‡ The University of Tokyo.

(1) For Fe: (a) Norman, R. E.; Yan, S.; Que, L., Jr.; Backes, G.; Ling, J.; Sanders-Loehr, J.; Zhang, J. H.; O'Conner, C. J. *J. Am. Chem. Soc.* **1990**, *112*, 1554−1562. (b) Ménage, S.; Zang, Y.; Hendrich, M. P.; Que, L., Jr. *J. Am. Chem. Soc.* **1992**, *114*, 7786−7792. (c) Zang, Y.; Elgren, T. E.; Dong, Y.; Que, L., Jr. *J. Am. Chem. Soc.* **1993**, *115*, 811−813. (d) Leising, R. A.; Kim, J.; Pérez, M.; Que, L., Jr. *J. Am. Chem. Soc.* **1993**, *115*, 9524−9530. (e) Kojima, T.; Leising, R. A.; Yan, S.; Que, L., Jr. *J. Am. Chem. Soc.* **1993**, *115*, 11328−11335. (f) Chiou, Y.-M.; Que, L., Jr. *J. Am. Chem. Soc.* **1995**, *117*, 3999−4013. (g) Dong, Y.; Fujii, H.; Hendrich, M. P.; Leising, R. A.; Pan, G.; Randall, C. R.; Wilkinson, E. C.; Zang, Y.; Que, L., Jr.; Fox, B. G.; Kauffmann, K.; Münck, E. *J. Am. Chem. Soc.* **1995**, *117*, 2778−2792. (h) Que, L., Jr.; Dong, Y. *Acc. Chem. Res.* **1996**, *29*, 190−196. (i) Zang, Y.; Kim, J.; Dong, Y.; Wilkinson, E. C.; Appleman, E. H.; Que, L., Jr. *J. Am. Chem. Soc.* **1997**, *119*, 4197−4205.

(2) For Cu: (a) Jacobson, R. R.; Tyeklár, Z.; Farooq, A.; Karlin, K. D.; Liu, S.; Zubieta, J. *J. Am. Chem. Soc.* **1988**, *110*, 3690−3692. (b) Tyeklár, Z.; Jacobson, R. R.; Wei, N.; Murthy, N. N.; Zubieta, J.; Karlin, K. D. *J. Am. Chem. Soc.* **1993**, *115*, 2677−2689. (c) Harata, M.; Jitsukawa, K.; Masuda, H.; Einaga, H. *J. Am. Chem. Soc.* **1994**, *116*, 12079−12080. (d) Berreau, L. M.; Mahapatra, S.; Haften, J. A.; Young, V. G., Jr.; Tolman, W. B. *Inorg. Chem.* **1996**, *35*, 6639−6342. (e) Nagao, H.; Komeda, N.; Mukaida, M.; Suzuki, M.; Tanaka, K. *Inorg. Chem.* **1996**, *35*, 6809−6815.

(3) Sugimoto, H.; Kamei, M.; Umakoshi, K.; Sasaki, Y.; Suzuki, M. *Inorg. Chem.* **1996**, *35*, 7082−7088.

(4) Sugimoto, H.; Sasaki, Y. *Chem. Lett.* **1997**, 541−542.

S0020-1669(97)01049-5 CCC: $15.00
Published on Web 07/24/1998

For these purposes, bpy (2,2′-bipyridyl), trpy (2,2′:6′,2″-terpyridyl), phen (1,10-phenanthroline), and their derivatives have been employed because of the lower energy of the triplet states of the Ru(II) complexes; all of them act as bidentate π-acceptors. Ru(TPA derivatives) complexes have not yet been reported;[10] however, it is intriguing to explore molecular structures and chemical properties of Ru complexes with tightly bound tripodal pyridylamine ligands. In an attempt to construct a new category of Ru complexes with ligands with the π-acceptor and the σ-donor in the same molecule, we have embarked on studies of Ru complexes having TPA and its derivatives as ligands. As reported previously, we discovered that those Ru-TPA complexes could catalyze alkane functionalization with use of peroxides as cooxidants.[10] We describe herein the synthesis and characterization of novel Ru(II) and Ru(III) complexes with TPA and 5-Me$_3$-TPA (tris(5-methyl-2-pyridylmethyl)amine) to establish the structures of those complexes and understand their electronic characters.

Experimental Section

Materials and Synthesis. All chemicals were used as received without further purification. TPA·3HClO$_4$,[11] 5-Me$_3$-TPA,[1g] and *cis*-[RuCl$_2$(DMSO)$_4$][12] were synthesized according to literature methods. All NMR measurements were performed on JEOL GX-400 and EX-270 spectrometers. UV/vis absorption spectra were measured in CH$_3$CN on a Jasco Ubest-55 UV/vis spectrophotometer at room temperature. Infrared spectra were recorded as KBr disks in the range of 4000−400 cm^{-1} on a Jasco IR model 800 infrared spectrophotometer. FAB-MS spectra were measured on a JMS-SX/SX102A tandem mass spectrometer. Elemental analysis data for all compounds were obtained at the Service Center of the Elemental Analysis of Organic Compounds, Department of Chemistry, Kyushu University.

[RuCl(TPA)(DMSO)]ClO$_4$ (1). To a degassed solution of TPA·3HClO$_4$ (1.18 g, 2 mmol) and NEt$_3$ (0.607 g, 6 mmol) in MeOH (10 mL) was added *cis*-[RuCl$_2$(DMSO)$_4$] (0.84 g, 2 mmol) as solid. The mixture was refluxed for 4 h under N$_2$. Yellow precipitate was filtered, washed with MeOH, and then dried. The isolated yield was 0.52 g (45%). Anal. Calcd for C$_{20}$H$_{24}$N$_4$O$_5$Cl$_2$SRu: C, 39.74; H, 4.00; N, 9.27. Found: C, 39.65; H, 4.04; N, 9.24. ^{1}H NMR (CD$_3$CN): 3.419 (s, 6H, CH_3 of DMSO), 4.687 (s, 2H, CH_2 (axial)), 4.787 and 5.765 (ABq, J_{AB} = 15 Hz, 4H, CH_2 (equatorial)), 6.962 (d, J = 8 Hz, 1H, pyr-H3 (axial)), 7.167 (t, J = 6 Hz, 1H, pyr-H5 (axial)), 7.238 (t, J = 7 Hz, 2H, pyr-H5 (equatorial)), 7.496 (td, J = 8 and 2 Hz, 1H, pyr-H4 (axial)), 7.481 (dd, J = 8 and 8 Hz, 2H, pyr-H3 (equatorial)), 7.744 (td, J = 8 and 2 Hz, 2H, pyr-H4 (equatorial)), 8.708 (d, J = 5 Hz, 2H, pyr-H6 (equatorial)), 9.813 (d, J = 5 Hz, 1H, pyr-H6 (axial)). FAB-MS: 505 (M^+), 427 ([M − DMSO]$^+$). Absorption maxima (λ_{max}, nm): 414, 346.

[RuCl(5-Me$_3$-TPA)(DMSO)]ClO$_4$·H$_2$O (2·H$_2$O). To a degassed mixture of 5-Me$_3$-TPA (0.33 g, 1 mmol) and *n*-Bu$_4$NClO$_4$ (1.02 g, 3 mmol) in MeOH (20 mL) was added *cis*-[RuCl$_2$(DMSO)] (0.48 g, 1 mmol) as solid in portions. The yellow suspension was refluxed overnight to afford an orange solution. By cooling it down to room temperatures, yellow needle crystals were obtained. The crystals were filtered, washed with Et$_2$O, and dried in vacuo. Anal. Calcd for C$_{23}$H$_{30}$N$_4$Cl$_2$O$_5$SRu·H$_2$O: C, 41.57; H, 4.85; N, 8.43. Found: C, 41.51; H, 4.79; N, 8.41. The yield was 77% (0.50 g). ^{1}H NMR (CD$_3$CN): 2.228 (s, 6H, py-5-Me (equatorial)), 2.298 (s, 3H, py-5-Me (axial)), 2.843 (s, 6H, CH_3 of DMSO), 4.425 (s, 2H, CH_2 (axial)), 4.590 and 5.332 (ABq, J_{AB} = 15 Hz, 4H, CH_2 (equatorial)), 6.997 (d, 8 Hz, 1H, py-H3 (axial)), 7.286 (d, 8 Hz, 2H, py-H3 (equatorial)), 7.467 (dd, 8 and 2 Hz, 1H, py-H4 (axial)), 7.562 (dd, 8 and 2 Hz, 2H, py-H4 (equatorial)), 8.571 (s, 2H, py-H6 (equatorial)), 9.529 (s, 1H, py-H6 (axial)). Absorption maxima (λ_{max}, nm): 426 (sh), 361, 311 (sh).

[RuCl(TPA)]$_2$(ClO$_4$)$_2$·$^1/_2$CH$_3$CN (3·$^1/_2$CH$_3$CN). To a degassed solution of TPA·3HClO$_4$ (0.68 g, 1.15 mmol) and NEt$_3$ (0.58 g, 5.73 mmol) in MeOH (20 mL), was added a solution of RuCl$_3$·3H$_2$O (0.30 g, 1.15 mmol) in MeOH (20 mL) under N$_2$ via a cannula. The mixture was refluxed for 8 h, and brown precipitate was filtered off. The brown powder was washed with ether and dissolved into CH$_3$CN. Insoluble materials were filtered off through a Celite 535 column to obtain a reddish orange solution. The solvent was removed by rotatory evaporator, and the resultant orange powder of **2** was washed well with ether then dried. The isolated yield was 0.27 g (44%). Anal. Calcd for C$_{36}$H$_{36}$N$_8$Cl$_4$O$_8$Ru$_2$·$^1/_2$CH$_3$CN: C, 41.41; H, 3.52; N, 11.09. Found: C, 40.92; H, 3.54; N, 11.28. ^{1}H NMR (CD$_3$CN): 4.251 (s, 2H, CH_2 (axial)), 4.560 and 5.111 (ABq, J_{AB} = 15 Hz, 4H, CH_2 (equatorial)), 6.820 (d, J = 8 Hz, 1H, pyr-H3 (axial)), 6.864 (t, J = 6 Hz, 2H, pyr-H5 (equatorial)), 6.962 (t, J = 7 Hz, 1H, pyr-H5 (axial)), 7.316 (td, J = 8 and 1 Hz, 1H, pyr-H4 (axial)), 7.436 (d, J = 7 Hz, 2H, pyr-H3 (equatorial)), 7.663 (td, J = 8 and 2 Hz, 2H, pyr-H4 (equatorial)), 8.407 (dd, J = 6 and 1 Hz, 2H, pyr-H6 (equatorial)), 8.795 (d, J = 5 Hz, 1H, pyr-H6 (axial)). Absorption maxima (λ_{max}, nm): 430, 355 (sh).

[RuCl(5-Me$_3$-TPA)]$_2$(ClO$_4$)$_2$·H$_2$O (4·H$_2$O). To a degassed solution of RuCl$_3$·3H$_2$O (0.523 g, 2 mmol) in MeOH (20 mL) was added via cannula a mixture including 5-Me$_3$-TPA (0.665 g, 2 mmol), NEt$_3$ (1.012 g, 10 mmol), and NaClO$_4$ (1.22 g, 10 mmol) under N$_2$. The mixture was refluxed for 12 h and then filtered to obtain yellow-brown powder. The crude product was dissolved into CH$_3$CN and filtered through a Celite 535 column to afford a reddish orange solution. An orange powder of **3** was obtained by removing CH$_3$CN and was washed with ether. The isolated yield was 0.28 g (24%). Anal. Calcd for C$_{42}$H$_{48}$N$_8$O$_8$Cl$_4$Ru$_2$·H$_2$O: C, 43.68; H, 4.36; N, 9.70. Found: C, 43.94; H, 4.61; N, 9.77. ^{1}H NMR (CD$_3$CN): 1.880 (s, CH_3 (equatorial)), 2.092 (s, CH_3 (axial)), 4.200 (s, 2H, CH_2 (axial)), 5.098 and 4.481 (AB$_q$, J_{AB} = 15 Hz, 4H, CH_2 (equatorial)), 6.698 (d, J = 8 Hz, 1H, pyr-H3 (axial)), 7.144 (d, J = 8 Hz, 1H, pyr-H4 (axial)), 7.318 (d, J = 8 Hz, 2H, pyr-H3 (equatorial)), 7.508 (d, J = 8 Hz, 2H, pyr-H4 (equatorial)), 8.265 (s, 2H, pyr-H6 (equatorial)), 8.621 (s, 1H, pyr-H6 (axial)). Absorption maxima (λ_{max}, nm): 432, 357(sh).

[RuCl$_2$(TPA)]ClO$_4$·H$_2$O (5·H$_2$O). To a refluxed solution of RuCl$_3$·3H$_2$O (0.52 g, 2 mmol) in EtOH (150 mL) was added a mixture containing TPA·3HClO$_4$ (1.18 g, 2 mmol) and NaOH (0.184 g, 4.6 mmol) in EtOH (150 mL). The mixture was refluxed for 22 h, and an orange precipitate emerged. The precipitate was filtered, washed with ether, and then dried. The isolated yield was 1.07 g (85%). Anal. Calcd for C$_{18}$H$_{18}$N$_4$ClO$_4$Ru·H$_2$O: C, 37.28; H, 3.48; N, 9.66. Found: C, 37.09; H, 3.14; N, 9.45. Absorption maxima (λ_{max}, nm): 434, 352 (sh), 322.

[RuCl$_2$(5-Me$_3$-TPA)]ClO$_4$ (6). To a refluxed solution of RuCl$_3$·3H$_2$O (0.52 g, 2 mmol) in EtOH (100 mL) was added a mixture including 5-Me$_3$-TPA (0.67 g, 2 mmol) and HClO$_4$ (60%, 0.33 g, 2 mmol) in EtOH (40 mL). The mixture was kept refluxed for 24 h. After the solvent was removed by rotatory evaporator, a small volume of CH$_3$CN was added and insoluble materials were filtered off to obtain an orange solution. An orange powder of **5** was obtained by drying up the solvent. The isolated yield was 0.977 g (81%). Anal. Calcd for C$_{21}$H$_{24}$N$_4$Cl$_3$O$_4$Ru: C, 41.77; H, 4.01; N, 9.28. Found: C, 41.88; H, 4.31; N, 9.26. Absorption maxima (λ_{max}, nm): 426, 354 (sh), 324, 465 (sh).

X-ray Crystallographic Data Collections. A single crystal of **2** having one MeOH molecule of crystallization was obtained by recrystallization from a hot MeOH solution of **2**. The ^{1}H NMR spectrum of **2** in CD$_3$CN indicated the existence of one MeOH molecule (3.264 ppm, d, 5 Hz, 3H). The crystal of **2** (0.20 × 0.15 × 0.30 mm^3)

(5) Juris, A.; Balzani, V.; Barigelletti, F.; Campagna, S.; Belser, P.; von Zelewsky, A. *Coord. Chem. Rev.* **1988**, *84*, 85−277.
(6) Krantz, E.; Ferguson, J. *Prog. Inorg. Chem.* **1989**, *37*, 293−390.
(7) Dodsworth, E. S.; Lever, A. B. P *Chem. Phys. Lett.* **1986**, *124*, 152−158.
(8) Hecker, C. R.; Fanwick, P. E.; McMillin, D. R. *Inorg. Chem.* **1991**, *30*, 659−666.
(9) Meyer, T. J. *Acc. Chem. Res.* **1978**, *11*, 94−100.
(10) Preliminary results have been reported: Kojima, T. *Chem. Lett.* **1996**, 121−122.
(11) (a) Anderegg, G.; Wenk, F. *Helv. Chim. Acta* **1967**, *50*, 2330−2332. (b) Gafford, B. G.; Holewerda, R. A. *Inorg. Chem.* **1989**, *28*, 60−66.
(12) James, B. R.; Ochiai, E.; Rempel, G. I. *Inorg. Nucl. Chem. Lett.* **1971**, *7*, 781−784.

Table 1. Crystallographic Data for $[RuCl(5\text{-}Me_3\text{-}TPA)(DMSO)]ClO_4 \cdot CH_3OH$ (**2**), $[RuCl(TPA)]_2(ClO_4)_2 \cdot CH_3CN$ (**3**), and $[RuCl_2(TPA)]ClO_4$ (**5**)[a]

	2	**3**	**5**
empirical formula	$C_{24}H_{34}N_4SO_6Cl_2Ru$	$C_{38}H_{39}N_9O_8Cl_4Ru_2$	$C_{18}H_{18}N_4O_4Cl_3Ru$
fw	678.59	1093.73	561.79
crystal system	monoclinic	monoclinic	orthorhombic
a, Å	10.680(9)	13.977(4)	15.527(4)
b, Å	12.363(4)	21.991(5)	15.823(2)
c, Å	22.299(6)	15.651(6)	8.782(2)
β, deg	95.07(4)	113.43(2)	
V, Å^3	2933(2)	4414(2)	2157.5(7)
space group	$P2_1/c$	*C2/c*	$P2_12_12_1$
Z	4	4	4
D_{calcd}, g/cm^3	1.537	1.646	1.729
μ (Mo Kα), cm^{-1}	8.31	9.87	11.31
R (R_w)[b,c] (%)	4.5(4.9)	5.6 (3.0)	3.7 (1.8)

[a] $T = 293$ K; Mo Kα radiation ($\lambda = 0.7107$ Å). [b] $R = \sum||F_o| - |F_c||/\sum|F_o|$. [c] $R_w = \{\sum[w(|F_o| - |F_c|)^2]/\sum[w|F_o|^2]\}^{1/2}$.

was efflorescent and therefore mounted in a glass capillary. All measurements were made on a Rigaku AFC-7R diffractometer at 23 ± 1 °C with graphite-monochromated Mo Kα radiation ($\lambda = 0.7107$ Å) at Kyushu University. Cell constants and orientation matrixes for data collection were obtained from a least-squares refinement using the setting angles of 25 carefully centered reflections in the range $28.49 < 2\theta < 31.59°$. The data collection was made with the $\omega-2\theta$ scan to a maximum 2θ value of 50.0°. Three standard reflections were monitored after every 150 reflections to indicate no significant decay in the intensities. Data were corrected for Lorentz−polarization effects and for absorption through azimuthal scans.

A single crystal of **3** having one solvent molecule (CH_3CN) of crystallization suitable for X-ray analysis was obtained by recrystallization from a CH_3CN solution under reduced pressure. X-ray diffraction data were collected on a block-shaped orange crystal with dimensions $0.40 \times 0.50 \times 0.15$ mm^3 on a Rigaku AFC-7R diffractometer at 20 ± 1 °C with a graphite-monochromated Mo Kα ($\lambda = 0.7107$ Å) radiation at the Graduate School of Chemistry and Biotechnology, University of Tokyo. Cell constants and orientation matrixes for data collection were obtained from a least-squares refinement using the setting angles of 25 carefully centered reflections in the range $35.75 < 2\theta < 38.48°$. The data collection was made with the $\omega-2\theta$ scan to a maximum 2θ value of 55.0°. Three standard reflections were monitored after every 150 reflections to indicate no significant decay in the intensities. Data were corrected for Lorentz−polarization effects and for absorption through azimuthal scans.

A single crystal of **5** having no solvent molecule (Anal. Calcd for $C_{18}H_{18}N_4Cl_3O_4Ru$: C, 38.48; H, 3.23; N, 9.97. Found: C, 38.53; H, 3.19; N, 9.97) was obtained by recrystallization from 2 M HCl. X-ray diffraction data were collected on a block-shaped orange crystal with dimensions $0.20 \times 0.50 \times 0.30$ mm^3 on a Rigaku AFC-7R diffractometer with a graphite-monochromated Mo Kα ($\lambda = 0.7107$ Å) radiation at the Graduate School of Chemistry and Biotechnology, University of Tokyo. Cell constants and orientation matrixes for data collection were obtained from a least-squares refinement using the setting angles of 25 carefully centered reflections in the range $34.39 < 2\theta < 39.58°$. The data were collected at 20 ± 1 °C using $\omega-2\theta$ scan to a maximum 2θ value of 55.0°. The intensities of three representative reflections were measured after every 150 reflections to ascertain crystal integrity; no decay of intensity was observed. Data were corrected for Lorentz−polarization effects and for absorption through azimuthal scans. Pertinent crystallographic data and experimental conditions are summarized in Table 1.

Solution and Refinement of Structures. The structures were solved by heavy-atom Patterson methods and expanded using Fourier techniques. All non-hydrogen atoms were refined anisotropically. Refinement was carried out with full-matrix least-squares on *F* with scattering factors from reference and included anomalous dispersion effects. All calculations were performed using the teXsan crystallographic software package.[13] The atomic scattering factors were taken from ref 14, and anomalous dispersion effects were included; the values for $\Delta f'$ and $\Delta f''$ were taken from ref 15. The hydrogen atoms of **2** were refined, but their isotropic thermal factors were held fixed. The hydrogen atoms of **3** and **5** were included in the final least-squares but not refined. A perchlorate anion (for **2** and **3**) and the MeOH (for **2**) or the CH_3CN (for **3**) molecule were found to be disordered. The final positional parameters, thermal parameters, and complete listings of bond lengths and angles are included in the Supporting Information.

Cyclic Voltammetry. All cyclic voltammograms were recorded on an HECS 312B dc pulse polarograph (Fuso Electrochemical System) attached to an HECS 321B potential sweep unit of the same manufacture. A platinum disk (3 mm o.d.) was employed as a working electrode, a platinum coil as a counter electrode, and silver/silver nitrate ($Ag/AgNO_3$) electrode as a reference electrode, respectively. All measurements were carried out in CH_3CN containing 0.1 M $[(n\text{-}Bu)_4N]ClO_4$ as a supporting electrolyte under N_2 at ambient temperatures. The redox potentials were determined relative to ferrocene/ferrocenium couple as a reference (0 V).

Results

Synthesis. A series of Ru(II) and Ru(III) complexes were synthesized, with tripodal tetradentate TPA and 5-Me_3-TPA as ligands in moderate to high yields. A schematic description of their structures is shown in Figure 1. Concerning the synthesis of monomeric $[RuCl(TPA)(DMSO)]ClO_4$ (**1**) and $[RuCl(5\text{-}Me_3\text{-}TPA)(DMSO)]ClO_4$ (**2**) containing an S-bound DMSO molecule, the reaction proceeded via ligand substitution between the three originally bound monodentate DMSO molecules and one Cl^- ligand in *cis*-$[RuCl_2(DMSO)_4]$ and one tetradentate TPA or 5-Me_3-TPA due to chelating effect. For these compounds, there are two isomers for each; one has chloride trans to axial pyridine moiety and the other has that trans to the tertiary amino group. However, the isolated product showed only one set of signals for TPA or 5-Me_3-TPA and one singlet for the DMSO ligand (vide infra), suggesting that one isomer could be obtained selectively.[16]

A new bis-μ-chloro Ru(II) dimer $[RuCl(TPA)]_2(ClO_4)_2$ (**3**) was synthesized from the reaction of $TPA \cdot 3HClO_4$ with $RuCl_3 \cdot 3H_2O$ in MeOH in the presence of NEt_3 as a base. We examined some reaction conditions to reveal that it was indispensable for the formation of **2** to use MeOH as the solvent and NEt_3 as the

(13) *TeXsan: Crystal Structure Analysis Package*; Molecular Structure Corporation: The Woodlands, TX, 1985 and 1992.

(14) *International Tables for X-ray Crystallography*; Kynoch Press: Birmingham, England, 1974; Vol. IV.

(15) *International Tables for X-ray Crystallography*; Kluwer Academic Publishers: Boston, MA, 1992; Vol. C.

(16) After our submission of the manuscript, Yamaguchi and co-workers reported the crystal structure of **1**; it is structure (a) in Figure 1. ^1H NMR data for the complex is consistent with those of **1** in Table 5. Yamaguchi, M.; Kousaka, H.; Yamagishi, T. *Chem. Lett.* **1997**, 769−770.

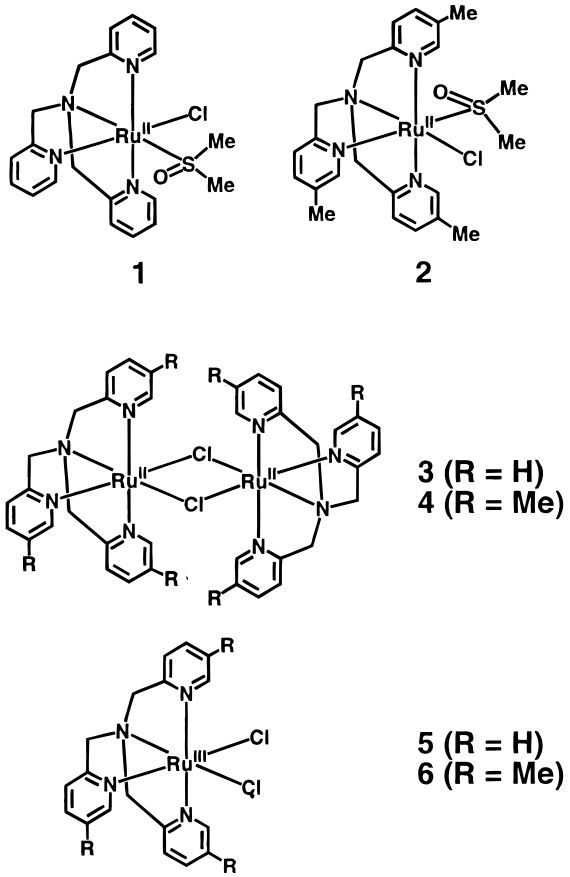

Figure 1. Structures of complexes **1**−**6**.

Table 2. Selected Bond Lengths (Å) and Angles (deg) for [RuCl(5-Me$_3$-TPA)(DMSO)]ClO$_4$·CH$_3$OH (**2**)

Ru−Cl1	2.423(2)	Cl1−Ru−S1	87.36(7)
Ru−S1	2.236(2)	Cl1−Ru−N1	174.4(1)
Ru−N1	2.062(4)	Cl1−Ru−N2	93.6(1)
Ru−N2	2.104(5)	Cl1−Ru−N3	100.3(1)
Ru−N3	2.066(4)	Cl1−Ru−N4	97.1(1)
Ru−N4	2.090(4)	S1−Ru−N1	98.0(1)
S1−O1	1.485(4)	S1−Ru−N2	174.9(1)
S1−C22	1.787(7)	S1−Ru−N3	91.3(2)
S1−C23	1.764(9)	S1−Ru−N4	93.5(1)
N1−C1	1.496(7)	N1−Ru−N2	81.2(2)
N1−C8	1.489(7)	N1−Ru−N3	83.6(2)
N1−C15	1.526(7)	N1−Ru−N4	81.0(2)
N2−C2	1.334(7)	N2−Ru−N3	83.6(2)
N2−C6	1.350(8)	N2−Ru−N4	91.3(2)
N3−C9	1.334(6)	N3−Ru−N4	162.1(2)
N3−C13	1.377(7)	Ru−S1−O1	119.1(2)
N4−C16	1.355(7)	Ru−S1−C22	111.4(2)
N4−C20	1.340(7)	Ru−S1−C23	106.1(4)

base: The dimer could not be obtained from either reaction in CH_3CN or EtOH or in MeOH with NaH as a base. This suggests that reduction of the Ru center is effectively carried out by the combination of MeOH and NEt_3, though the mechanism is not clear at this point. Similarly, [RuCl(5-Me$_3$-TPA)]$_2$(ClO$_4$)$_2$ (**4**) having 5-Me$_3$-TPA in place of TPA was synthesized in the same method, though the isolated yield was lower than that of **3** due to its higher solubility toward organic solvents. The purification of **3** and **4** could be done well by passing the CH_3CN solutions through a Celite column to remove green Ru(III) compounds and insoluble brown materials.

To prepare Ru^{III}-TPA and 5-Me$_3$-TPA complexes, we found that the dropwise addition of the ligand solution in EtOH to the refluxing solution of $RuCl_3$·3H_2O in EtOH gave almost quantitative formation of [Ru^{III}Cl$_2$(L)]$^+$ species. The procedure

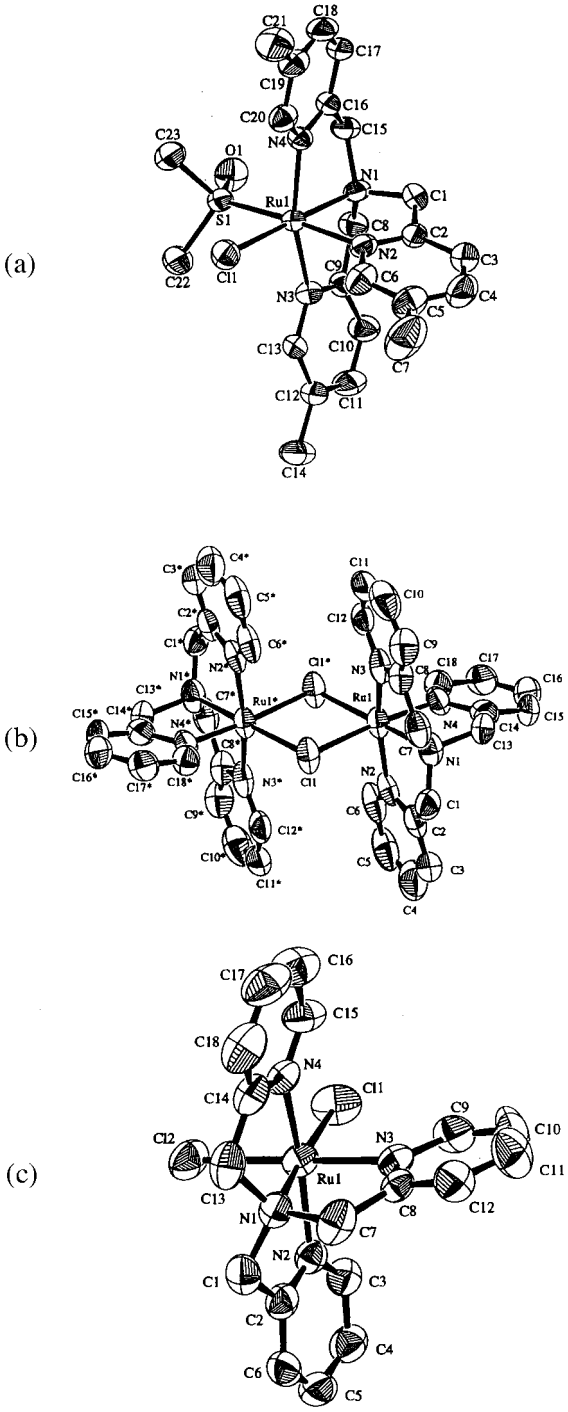

Figure 2. ORTEP drawings of cations of (a) **2**, (b) **3**, and (c) **5**. Thermal elipsoids are drawn at the 50% probability level.

is a modified method of that reported by Che and co-workers.[17] It is important to reflux the EtOH solution of $RuCl_3$ salt prior to react with ligand because a commercially available $RuCl_3$·3H_2O is inevitably contaminated by Ru(IV) compounds which can be reduced to Ru(III) by the procedure.[18] This method allowed us to synthesize monomeric Ru(III) complexes [RuCl$_2$(TPA)]ClO$_4$ (**5**) in the 85% isolated yield and [RuCl$_2$(5-Me$_3$-TPA)]ClO$_4$ (**6**) in the 81% yield. Note that NaOH should be used in place of NEt_3 to render TPA an acid-free form.

(17) Che, C.-M.; Yam, V. W.-W.; Mak, T. C. W. *J. Am. Chem. Soc.* **1990**, *112*, 2284−2291.
(18) Emerson, J.; Clarke, M. J.; Ying, W.-L.; Sanadi, D. R. *J. Am. Chem. Soc.* **1993**, *115*, 11799−11805.

Table 3. Selected Bond Lengths (Å) and Angles (deg) for $[RuCl(TPA)]_2(ClO_4)_2 \cdot CH_3CN$ (**3**)

Ru···Ru	3.648(2)	Cl−Ru−Cl′	84.04(7)
Cl···Cl′	3.286(4)	Ru−Cl−Ru′	95.96(7)
Ru−Cl	2.458(2)	Cl−Ru−N(1)	94.3(2)
Ru−Cl′	2.451(2)	Cl−Ru−N(2)	91.2(2)
Ru−N(1)	2.037(6)	Cl−Ru−N(3)	87.1(2)
Ru−N(2)	2.054(7)	Cl−Ru−N(4)	175.7(2)
Ru−N(3)	2.047(7)	Cl′−Ru−N(1)	177.8(2)
Ru−N(4)	2.025(6)	Cl′−Ru−N(2)	98.2(2)
N(1)−C(1)	1.493(9)	Cl′−Ru−N(3)	97.5(2)
N(1)−C(7)	1.493(9)	Cl′−Ru−N(4)	97.3(2)
N(1)−C(13)	1.539(8)	N(1)−Ru−N(2)	83.2(3)
N(2)−C(2)	1.347(9)	N(1)−Ru−N(3)	81.1(3)
N(2)−C(6)	1.342(9)	N(1)−Ru−N(4)	84.5(2)
N(3)−C(8)	1.321(8)	N(2)−Ru−N(3)	164.0(3)
N(3)−C(12)	1.374(9)	N(2)−Ru−N(4)	84.5(2)
N(4)−C(14)	1.376(8)	N(3)−Ru−N(4)	96.8(2)
N(4)−C(18)	1.317(8)		

Molecular Structure of Compounds 2, 3, and 5. A single crystal of **2**·CH_3OH was obtained by recrystallization from hot MeOH solution. An ORTEP drawing is shown in Figure 2a with atom numbering scheme. Selected bond lengths and angles are listed in Table 2.

Compound **2** was crystallized in the space group $P2_1/c$. The Ru(II) center was coordinated by four nitrogens of 5-Me_3-TPA, by Cl^-, and by a DMSO molecule which bound through the S atom. The geometry of **2** was revealed to be that the DMSO molecule binds to the Ru center at the site trans to pyridine and that Cl^- is trans to the tertiary amino group of 5-Me_3-TPA. This isomer was formed exclusively. Bond length of Ru−N1-(tertiary amino group) was 2.062(2) Å, and for pyridine moieties, 2.104(5) Å of Ru−N2 (trans to S atom of DMSO), 2.066(4) and 2.090(4) Å for Ru−N3 and Ru−N4 which were trans to each other, respectively. The angle ∠N3−Ru−N4 was 162.1(2)°, showing that the geometry around the Ru center was a distorted octahedron. The bond length of Ru−S bond was 2.236(2) Å, which was much shorter than those of Ru−DMSO complexes reported by Alessio and co-workers.[19] The bond length of S−O in DMSO ligand was 1.485(4) Å, which was longer than that of free DMSO molecule (1.47 Å)[20] and longer than those found in Ru(II) complexes having S-bonded DMSO ligands reported by Alessio and co-workers.[19] This is due to a strong π-back-donation from dπ of Ru(II) ion to pπ^* of S═O bond (vide infra).

A single crystal of **3** was obtained by the recrystallization from concentrated MeCN solution under reduced pressure. The crystal structure of **3** is shown in Figure 2b with atom labeling scheme. Selected bond lengths and angles are listed in Table 3.

The compound **3** was crystallized in the space group $C2/c$, having the center of symmetry at the midway between Cl and Cl′. Each Ru(II) center in **3** had an octahedral geometry with four sites for TPA and two for bridging chloride anions. Meyer and co-workers have reported the synthesis of a bis-μ-chloro Ru(II) dimer, $[RuCl(bpy)_2]_2^{2+}$; however, the structure has not been determined.[21] The separation between two ruthenium ions was 3.648(2) Å, and that between two chlorides was 3.286(2) Å, indicating no direct Ru···Ru and Cl···Cl interactions. The geometry of the Ru_2Cl_2 core was similar to those of reported structures such as $\{RuCl_2(NO)[(EtO)_2PO]_2H\}_2$,[22] $[(PPh_3)Ru(DPF)(\mu\text{-}Cl)Cl]_2$ (DPF = 3,3′,4,4′-tetramethyl-1,1′-diphosphaferrocene),[23] and $[Ru_2Cl_2(\eta^6\text{-hexamethylbenzene})_2]$,[24] which were determined in the space group of $P\bar{1}$ with the center of symmetry at similar positions. The pyridine rings of the TPA ligand were divided into two types: two pyridine moieties were trans to each other, namely *equatorial*, and one is trans to the μ-Cl^- ligand, namely *axial*. The two equatorial pyridine arms caused distortion of the octahedron of the ruthenium center having a bond angle ∠N2−Ru−N3 = 164.0(3)°. The bond distance of Ru−Cl (trans to pyridine) was 2.458(2) Å, a little longer than that of Ru−Cl′ (trans to the tertiary amino group) which was 2.451(2) Å. This is due to a stronger trans influence of pyridine than that of the tertiary amino group.[25] Pyridine moieties of the TPA ligand showed remarkable difference between equatorial pyridines and axial pyridine: The equatorial ones had similar distances of 2.054(7) Å for Ru−N(2) and 2.047(7) Å for Ru−N(3); the axial one which is trans to Cl^- had a shorter bond length of 2.025(7) Å for Ru−N(4). This tendency has shown in $[RuCl_2(bpy)_2]$,[26] for which pyridine nitrogen trans to Cl^- has shorter bond distance than that of pyridine trans to another pyridine. The bond length of Ru−N1(tertiary amino group) was 2.037(6) Å, which was much shorter than those in [Ru(1,4,8,11-tetrakis(2-pyridylmethyl)-1,4,8,11-teraazacyclotetradecaneH)]$^{3+}$ (2.264(2)−2.105(3) Å)[27] and $[Ru(baia)(bpy)]^{2+}$ (2.119(10) Å).[28]

Table 4. Selected Bond Lengths (Å) and Angles (deg) for $[RuCl_2(TPA)]ClO_4$ (**5**)

Ru(1)−Cl(1)	2.330(2)	Cl(1)−Ru(1)−Cl(2)	91.21(7)
Ru(1)−Cl(2)	2.357(2)	Cl(1)−Ru(1)−N(1)	175.9(2)
Ru(1)−N(1)	2.068(5)	Cl(2)−Ru(1)−N(3)	175.0(2)
Ru(1)−N(2)	2.074(5)	N(1)−Ru(1)−N(2)	81.3(2)
Ru(1)−N(3)	2.087(6)	N(1)−Ru(1)−N(3)	82.8(2)
Ru(1)−N(4)	2.073(5)	N(1)−Ru(1)−N(4)	81.8(2)
N(1)−C(1)	1.516(8)	N(2)−Ru(1)−N(4)	163.1(2)
N(1)−C(7)	1.498(8)	Ru(1)−N(1)−C(1)	105.8(4)
N(1)−C(13)	1.506(9)	Ru(1)−N(1)−C(7)	110.0(4)
N(2)−C(2)	1.354(8)	Ru(1)−N(1)−C(13)	106.4(4)
N(2)−C(3)	1.306(8)	Ru(1)−N(2)−C(2)	112.4(5)
N(3)−C(8)	1.365(7)	Ru(1)−N(2)−C(3)	127.5(5)
N(3)−C(9)	1.344(8)	Ru(1)−N(3)−C(8)	113.9(5)
N(4)−C(14)	1.384(8)	Ru(1)−N(3)−C(9)	129.1(6)
N(4)−C(15)	1.315(8)	Ru(1)−N(4)−C(14)	111.7(5)
		Ru(1)−N(4)−C(15)	128.4(5)

A single crystal of compound **5** was obtained by recrystallization from 2 M HCl, and the molecular structure was determined by X-ray crystallography. The structure of the cation is depicted in Figure 2c with atom numbering scheme, and selected bond lengths and angles are listed in Table 4. The geometry around Ru(III) center was slightly distorted octahedral, having ∠N2−Ru−N4 = 163.1(2)°. The bond distances between pyridine nitrogens and the Ru center were longer than those found in **3**: 2.087(6) Å for Ru−N3 which is trans to Cl^-,

(19) (a) Alessio, E.; Milani, B.; Bolle, M.; Mestroni, G.; Faleschini, P.; Todone, F.; Geremia, S.; Calligaris, M. *Inorg. Chem.* **1995**, *34*, 4722−4734. (b) Alessio, E.; Mestroni, G.; Nardin, G.; Attia, W. M.; Calligaris, M.; Sava, G.; Zorzet, S. *Inorg. Chem.* **1988**, *27*, 4099−4106.

(20) *Kagaku Binrann, Kisohen*, The Chemical Society of Japan; Maruzen: Tokyo, Japan; 1966; Vol. II, p 1222.

(21) Johnson, E. C.; Sullivan, B. P.; Salmon, D. J.; Adeyemi, S. A.; Meyer, T. J. *Inorg. Chem.* **1978**, *17*, 2211−2215.

(22) Southern, T. G.; Dixneuf, P. H.; Le Marouille, J.-Y.; Grandjean, D. *Inorg. Chem.* **1979**, *18*, 2987−2991.

(23) Deschamps, B.; Mathey, F.; Fischer, J.; Nelson, J. H. *Inorg. Chem.* **1984**, *23*, 3455−3462.

(24) McCormick, F. B.; Gleason, W. B. *Acta Crystallogr.* **1988**, *C44*, 603−605.

(25) Huheey, J. E. *Inorganic Chemistry*, 3rd ed.; Harper & Row Publishers: New York, 1983.

(26) Eggleston, D. S.; Goldsby, K. A.; Hodgson, D. J.; Meyer, T. J. *Inorg. Chem.* **1985**, *24*, 4573−4580.

(27) Che, C.-M.; Tang, W.-T.; Mak, T. C. W. *J. Chem. Soc., Dalton Trans.* **1988**, 2879−2883.

(28) Sakai, K.; Yamada, Y.; Tsubomura, T. *Inorg. Chem.* **1996**, *35*, 3163−3172.

Table 5. ^{1}H NMR Data (Measured in CD_3CN at Room Temperature)

	chemical shift assignments, ppm (*J*, Hz)					
	C*H*$_2$	pyr-H3	pyr-H4	pyr-H5	pyr-H6	Me
TPA	3.792 (s)	7.575 (d, 8)	7.688 (td, 8, 2)	7.170 (t, 6)	8.460 (d, 4)	
1	4.687 (ax, s)	6.962 (ax, d, 8)	7.496 (ax, td, 8, 2)	7.167 (ax, t, 6)	9.813 (ax, d, 5)	3.419 (DMSO, s)
	4.787, 5.765 (eq, ABq, 15)	7.481 (eq, dd, 8, 2)	7.744 (eq, td, 8, 2)	7.238 (eq, t, 7)	8.708 (eq, d, 5)	
3	4.251 (ax, s)	6.820 (ax, d, 8)	7.316 (ax, td, 8, 1)	6.962 (ax, t, 7)	8.795 (ax, d, 5)	
	4.560, 5.111 (eq, ABq, 15)	7.436 (eq, d, 7)	7.663 (eq, td, 8, 2)	6.864 (eq, t, 6)	8.407 (eq, dd, 6, 1)	
5-Me$_3$−TPA	3.707 (d, 2)	7.425−7.527 (m)			8.301 (d, 1)	2.266 (d, 2)
2	4.425 (ax, s)	6.997 (ax, d, 8)	7.467 (ax, dd, 8, 2)		9.529 (ax, s)	2.298 (ax, s)
	4.590, 5.332 (eq, ABq, 15)	7.286 (eq, d, 8)	7.562 (eq, dd, 8, 2)		8.571 (eq, s)	2.228 (eq, s)
						2.843 (DMSO, s)
4	4.220 (ax, s)	6.698 (ax, d, 8)	7.144 (ax, d, 8)		8.621 (ax, s)	2.092 (ax, s)
	4.481, 5.098 (eq, ABq, 15)	7.318 (eq, d, 8)	7.508 (eq, d, 8)		8.265 (eq, s)	1.880 (eq, s)

and 2.074(5) and 2.073(5) Å for Ru−N2 and Ru−N4, respectively, which are trans to each other. Comparing them with those of other related Ru(III) mononuclear complexes having pyridine derivatives revealed that the distances are slightly shorter than those found in $[Ru(N_4O)(H_2O)](ClO_4)_2$ (**7**) (2.083(5)−2.101(5) Å) as reported by Che and co-workers[17] and slightly longer than those of $[RuCl_2(bpy)_2]^+$ (2.045(5)−2.063(5) Å) as reported by Meyer and co-workers.[26] The tertiary amino nitrogen binds to the Ru(III) center (Ru−N1) with a distance of 2.068(5) Å, which is shorter than those in **7** (2.087(5) Å)[17] or *fac*-$[RuCl_3(trenH)]^+$ (2.126(6) Å).[28]

Spectroscopic Properties of Ru^{II}-TPA Complexes. ^{1}H NMR spectra of **1**−**4** were measured in CD_3CN and peak assignments were accomplished by integration of peak intensity and ^{1}H−^{1}H COSY spectroscopy. Peak assignments are listed in Table 5.

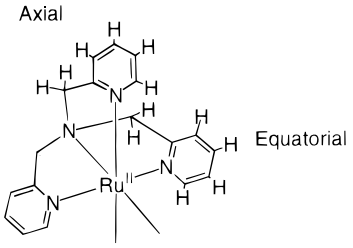

The ^{1}H NMR spectrum of **1** showed two sets of peaks for one axial pyridylmethyl arm and two equatorial pyridylmethyl arms and also a singlet peak at 3.419 ppm, which was assigned to the methyl groups of an S-bound DMSO molecule. For the methylene protons of the TPA ligand, two kinds of signals were observed: A singlet at 4.687 ppm was attributed to an axial C*H*$_2$ moiety; an AB quartet at 4.787 and 5.765 ppm (J_{AB} = 15 Hz) was ascribed to equatorial C*H*$_2$ moieties. As indicated in Table 5, methylene protons, equatorial pyridine protons, and axial pyr-H6's showed downfield shifts relative to those of free TPA; however, resonances due to other axial pyridyl protons were upfield-shifted. An NOE experiment was performed to consider which isomer was formed; irradiation at the singlet peak of methyl groups of DMSO ligand caused an intensity increase of 6 ± 1% for the equatorial H6 peak and 1 ± 1% for the axial one, suggesting the DMSO methyl groups should be far enough away from each H6 of pyridines.

The ^{1}H NMR spectrum of **2** was similar to that of **1** except for a singlet at 2.843 ppm assigned to the methyl group of an S-bound DMSO molecule, a singlet at 2.298 ppm for the 5-Me group of the axial pyridylmethyl arm, and a singlet at 2.228 ppm due to the 5-Me group of the equatorial pyridylmethyl arm.

Table 6. Redox Potentials of **1**−**6** Measured in CH_3CN at Ambient Temperatures under N_2[a]

complex	$E_{1/2}$ vs Fc/Fc$^+$ (V)[b]	
(a) Mononuclear Complexes		
	Ru^{II}/Ru^{III}	Ru^{III}/Ru^{IV}
$[RuCl(TPA)(DMSO)]^+$ (**1**)	0.61 (S-bound)	*c*
	0.04 (O-bound)[d]	
$[RuCl(5\text{-}Me_3\text{-}TPA)(DMSO)]^+$ (**2**)	0.52	*c*
$[RuCl_2(TPA)]^+$ (**5**)	−0.13	1.37
$[RuCl_2(5\text{-}Me_3\text{-}TPA)]^+$ (**6**)	−0.26	1.34
(b) Dinuclear Complexes		
	Ru^{II}Ru^{II}/Ru^{II}Ru^{III}	Ru^{II}Ru^{III}/Ru^{III}Ru^{III}
$[RuCl(TPA)]_2^{2+}$ (**3**)	0.22	0.71
$[RuCl(5\text{-}Me_3\text{-}TPA)]_2^{2+}$ (**4**)	0.17	0.66

[a] 0.1 M $[(n\text{-}Bu)_4N]ClO_4$ as an electrolyte. [b] Potentials were determined relative to Fc/Fc$^+$ couple as 0 V. [c] Not observed within the observed range (∼2 V). [d] This redox couple was not observed at the first sweep and emerged after the first oxidation process.

In the IR spectrum (KBr pellet) of **1**, an absorption observed at 1072 cm^{-1} was assigned to ν(S−O), which was a shoulder peak on strong ν(Cl−O) peaks of ClO_4^-. This assignment was made by comparing the IR spectrum of **1** with that of **4** and reported values (1096 cm^{-1}) for $[RuCl_2(CO)(py)_2(DMSO)]$.[19a] The IR spectrum of **2** showed ν(S−O) at 1070 cm^{-1}, which was almost the same in light of its resolution (4 cm^{-1}). Those absorption bands were lower than those observed for complexes reported by Alessio and co-workers[19] to represent that the S=O bonds in **1** and **2** were weakened to some extent.

In ^{1}H NMR spectrum of the bis-μ-chloro dimer **3**, the TPA moiety showed pattern similar to that of **1** as listed in Table 5. All methylene protons and pyr-H6 of the axial pyridine ring showed downfield shifts compared to the free TPA; in contrast, all other pyridine protons showed upfield shifts. A similar tendency was observed in the ^{1}H NMR spectrum of **4**, and 5-Me groups also showed upfield shifts compared to that of free 5-Me$_3$-TPA.

UV/vis spectroscopy was applied to complexes **1**−**6** to observe MLCT bands in CH_3CN solutions. Changing TPA to 5-Me$_3$-TPA gave no significant difference in MLCT bands due to Ru(dπ) → py(pπ*) transitions, suggesting π-acceptor character of both ligands would be comparable.

Cyclic Voltammetry. Cyclic voltammograms (CV) of **1**−**6** were obtained in CH_3CN with 0.1 M $[(n\text{-}Bu)_4N]ClO_4$ as an electrolyte at ambient temperatures under N_2. Redox potentials were measured relative to an $Ag/AgNO_3$ reference electrode and determined as potentials vs ferrocene/ferrocenium (Fc/Fc$^+$) redox couple as 0 V for each measurement. CV data are summarized in Table 6.

For mononuclear Ru(II) complex **1** with the S-bound DMSO ligand, originally one apparently reversible redox couple due

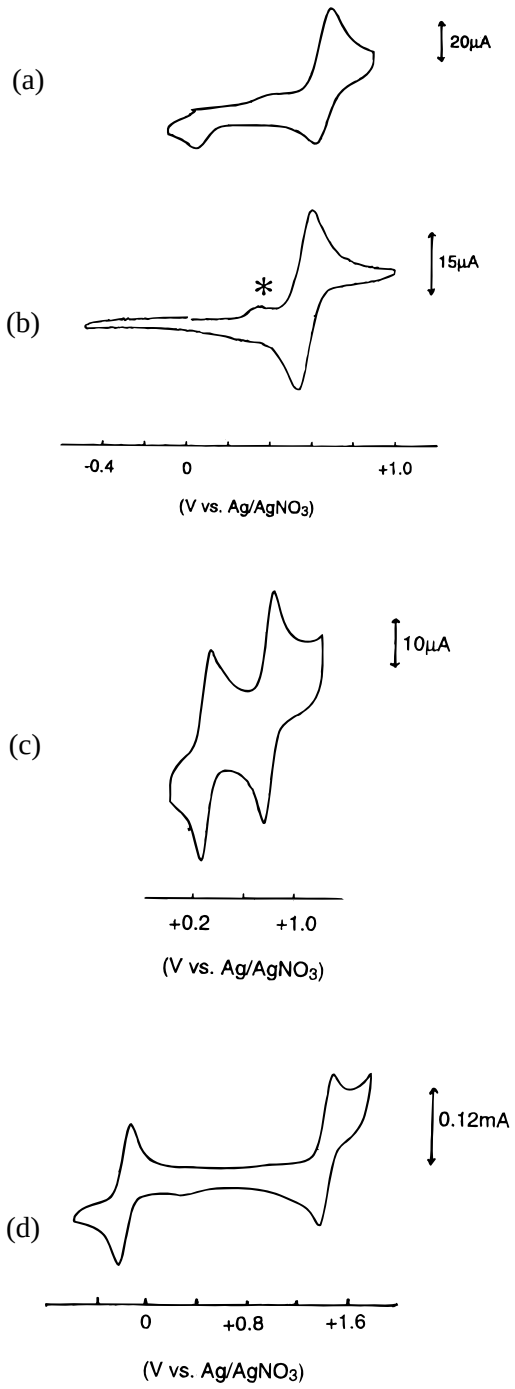

Figure 3. Cyclic voltammograms of **1** (trace (a)), **2** (trace (b)), **3** (trace (c)), and **5** (trace(d)) at ambient temperatures in CH_3CN (100 mV/s, 0.1 M TBA(ClO_4)). The asterisk in the trace (b) represents signal due to impurity in the solvent.

to the $Ru^{II}-Ru^{III}$ couple at +0.61 V was observed. After the second sweep, an additional reversible redox couple at +0.04 V was observed, as shown in Figure 3a. This negatively shifted wave is assigned to an isomer of **1** which has an O-bound DMSO ligand. Multiple sweeps of the solution of **1** increased the intensity of the +0.04 V redox wave. For this complex, no $Ru^{III}-Ru^{IV}$ redox couple was observed within the sweep range (from −2 to + 2V). The CV of **2** showed one reversible redox wave at +0.52 V, as shown in Figure 3b, which was negatively shifted relative to that of **1**. In the CV of **2** no other redox wave was observed to indicate that the stability of **2** is much higher than that of **1** in the electrochemical redox processes. This is due to electron-donating property of three methyl groups on pyridine rings to enrich the electron density at the Ru center. This lower potential for **2** is consistent with observations that **1** is not oxidized in aerobic solutions (DMSO, CH_3CN, MeOH, 2-propanol); however, **2** is oxidized in aerobic MeOH within 24 h.

Bis-μ-chloro dinuclear Ru(II) complexes **3** and **4** showed two reversible redox waves due to $Ru^{II}Ru^{II}-Ru^{II}Ru^{III}$ and $Ru^{II}Ru^{III}-Ru^{III}Ru^{III}$ couples. The CV trace for **3** is shown in Figure 3c as a representative. For complex **3**, they were observed at +0.22 and +0.71 V, respectively, and at +0.17 and +0.66 V for **4**. These observations are in sharp contrast to the fact that $[RuCl(bpy)_2]_2(PF_6)_2$ undergoes dissociation reaction in CH_3CN to form a mononuclear species which shows only one redox wave.[20] The stability of the mixed-valent $Ru^{II}Ru^{III}$ state can be represented by the comproportionation constant (K_{com}) defined by eq 1, where ΔE is the separation of two redox potentials mentioned above.

$$K_{com} = [Ru^{II}Ru^{III}]^2/[Ru^{II}Ru^{II}][Ru^{III}Ru^{III}] = \exp(F\Delta E/RT) \quad (1)$$

K_{com} values were determined to be 1.6×10^8 for **3** and 1.7×10^8 for **4**, which were comparable and showed no significant change by introducing the methyl groups. These K_{com} values are much larger than those found in μ-hydroxo dinuclear complexes[29] or Taube−Creutz type dimeric complexes.[30] Those are, however, much smaller than those observed for μ-oxo Ru(III) dimers which have larger separation between $Ru^{II}Ru^{III}-Ru^{III}Ru^{III}$ and $Ru^{III}Ru^{III}-Ru^{III}Ru^{IV}$ couples.[31] Therefore, it is indicated that the mixed valence state of the bis-μ-chloro dimers with the TPA derivatives is more stable than that of μ-hydroxo or Taube−Creutz type dimers but less stable than $Ru^{III}Ru^{IV}$ states of μ-oxo dimers.

Monomeric Ru(III) complexes **5** and **6** showed two reversible redox waves at −0.13 and +1.37 V for **5** and at −0.26 and +1.34 V for **6**, respectively. As a representative result, the CV of **5** is depicted in Figure 3d. The lower redox wave was assigned to a $Ru^{II}-Ru^{III}$ process and the higher to a $Ru^{III}-Ru^{IV}$ couple which was not observed for other complexes described in this paper. The introduction of methyl group at the 5-position of pyridine ring clearly lowers the potentials of each process as well as complexes described above. The two electron-donating choloride anions for one Ru(III) center lower the redox potentials compared with those of the bis-μ-chloro dimers in which two chlorides bind to two Ru(II) centers, to enable the electrochemical generation of the Ru(IV) state of the monomers.

Discussion

Synthesis of Ru(II) and Ru(III) Complexes. We established the selective synthesis of Ru(II) and Ru(III) complexes having TPA derivatives by changing starting materials and reaction conditions. The procedures described in this paper will supply a wide range of Ru complexes with TPA and related compounds and will be able to control the oxidation states of

(29) Zhang, S.; Shepherd, R. E. *Inorg. Chem.* **1994**, *33*, 5262−5270.
(30) (a) Sutton, J. E.; Sutton, P. M.; Taube, H. *Inorg. Chem.* **1979**, *18*, 1017−1021. (b) Richardson, D. E.; Taube, H. *Inorg. Chem.* **1981**, *20*, 1278−1285. (c) Richardson, D. E.; Taube, H. *J. Am. Chem. Soc.* **1983**, *105*, 40−51. (d) Creutz, C. *Prog. Inorg. Chem.* **1983**, *30*, 1−73. (e) Ram, M. S.; Haim, A. *Inorg. Chem.* **1991**, *30*, 1319−1325.
(31) (a) Schneider, R.; Weyhermüller, T.; Wieghardt, K.; Nuber, B. *Inorg. Chem.* **1993**, *32*, 4925−4934. (b) Sasaki, Y.; Suzuki, M.; Nagasawa, A.; Tokiwa, A.; Ebihara, M.; Yamaguchi, T.; Kabuto, C.; Ochi, T.; Ito, T. *Inorg. Chem.* **1991**, *30*, 4903−4908.

the Ru centers. To synthesize monomeric Ru(II) complexes, *cis*-[RuCl$_2$(DMSO)$_4$] works nicely as a starting material. This compound has been used to obtain many Ru(II) complexes including phosphorus-containing compounds.[32] Alessio and co-workers have studied substitution reactions of *cis*-[RuCl$_2$-(DMSO)$_4$] with imidazole to show that the substitution takes place at O-bound DMSO ligand which bind at trans to an S-bound DMSO first followed by another S-bonded DMSO trans to Cl$^-$, Cl$^-$ trans to an S-bound one.[33] The interaction between pyridyl group is stronger than that of the tertiary amino group due to the π-back-bonding from the Ru(II) center, as observed in the X-ray crystallography of **2** and **3**.

The formation of bis-μ-chloro Ru(II) dimers proceeds via the reduction of Ru(III) to Ru(II) by the combination of MeOH and NEt$_3$. These two are indispensable to generate the dimer as mentioned in the Results. This type of reduction of metal center has been observed in the reaction of Co^{III}−amine complexes in MeOH in the presence of NEt$_3$: in this case, a low-spin Co(III) center is reduced to be a high-spin Co(II) complex via electron transfer from MeOH after deprotonation by NEt$_3$.[34] The reaction mechanism of the formation of the dimer is not yet clear; however, a similar reaction would operate here. It is surprising that we could not observe the formation of mononuclear [RuCl$_2$(TPA)], similar to [RuCl$_2$(bpy)$_2$].

Mononuclear Ru(III) complexes are obtained in high yields. The formation of these complexes is almost stoichiometric, and the reaction is very clean. Compared with the synthesis of [RuCl$_2$(bpy)$_2$]Cl, the yields of **5** and **6** are much higher, and this is attributable to the fact that TPA and 5-Me$_3$-TPA are tetradentate ligands while bpy is bidentate. Therefore, **5** and **6** are much more stable than [RuCl$_2$(bpy)$_2$]Cl when isolated. However, we could not observe the formation of a bis-μ-chloro Ru(III) dimer which would be unstable due to its highly positive charge (+4), if it were formed. To crystallize these complexes, the solution should be acidified by 2 M HCl to avoid the dissociation of Cl$^-$ ligand. This procedure has been reported for the synthesis of [RuCl$_2$(TEPA)]$^+$ (TEPA = tris(2-(2-pyridyl)ethyl)amine) by Che and co-workers.[17] Meyer and co-workers used LiCl probably for this purpose to synthesize [RuCl$_2$(bpy)$_2$]Cl.[26] The Ru(III) complexes with tetradentate and tripodal TPA and 5-Me$_3$-TPA are very stable compared with a Ru(III) complex having tren (tris(2-aminoethyl)amine) in which one of three primary amino groups cannot bind to the Ru(III) center of [RuCl$_3$(trenH)]$^+$.[28] Such a tridentate situation of the tren ligand is ascribed to the steric constraint at the tertiary amino group toward two facially coordinated primary amino groups to set free the other primary amino group.

Structures of Ru Complexes. We revealed crystal structures of three new compounds, [RuCl(5-Me$_3$-TPA)(DMSO)]ClO$_4$ (**2**), [RuCl(TPA)]$_2$(ClO$_4$)$_2$ (**3**), and [RuCl$_2$(TPA)]ClO$_4$ (**5**). The structures of **4** and **6** were indicated to be identical to those of crystallographically characterized **3** and **5**, respectively.

Concerning the structure of complex **1**, there are two possibilities, as shown in Figure 1.

The structure of **2** was disclosed to have the DMSO binding to the Ru(II) center through the S atom at the position trans to the pyridine ring and Cl$^-$ at that trans to the tertiary amino group as described in Figure 1. According to ^{1}H NMR data cited in Table 5, the chemical shifts of the axial pyr-H6 for both **1** (9.813 ppm) and **2** (9.529 ppm) show large downfield shifts relative to those of each free ligand (8.460 and 8.301 ppm for TPA and 5-Me$_3$-TPA, respectively). A factor for this downfield shift is ascribed to the ring current of two equatorial pyridine rings which are located closely on both sides of the axial pyr-H6 hydrogen.

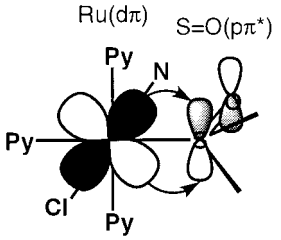

Figure 4. Schematic description of MO interaction between Ru(II) center and the S-bound DMSO molecule.

Table 7. Avarage Metal−Ligand Bond Lengths in the Complexes **3** and **5**

Ru−L	*d*(for **3**), Å	*d*(for **5**), Å	Δd,[a] Å
Ru−Cl(t-py)[b]	2.458	2.357	0.101
Ru−Cl(t-amine)[b]	2.451	2.330	0.121
Ru−N(py,t-Cl)[b]	2.025	2.087	−0.062
Ru−N(py, t-py)[b]	2.054, 2.047	2.074, 2.073	−0.027∼−0.019
Ru−N(amine)[b]	2.037	2.068	−0.031

[a] $\Delta d = d$(for **3**) $- d$(for **5**). [b] For definition of those listed, see text.

In the crystal structure of **2**, this property is reflected in the short Ru−S bond length (2.236(2) Å) and the elongated S═O bond (1.485(4) Å) of the DMSO ligand. The torsion angle among O1−S1−Ru1−N1 was 1.9(2)° which indicated that the S═O bond was almost in-plane to facilitate the π-back-bonding from the Ru center to the S═O moiety. A schematic molecular orbital interaction between them is described in Figure 4.

As for the structure of the bis-μ-chloro dimer **3**, the Ru$_2$Cl$_2$ core is completely in-plane and the bond length of Ru−Cl is longer for Ru−Cl (2.458(2) Å), which is trans to pyridine, than for Ru−Cl′ (2.451(2) Å), which is trans to the tertiary amino group. We conclude that there is no Ru−Ru interaction because of the large separation between them compared with complexes having such an interaction for which the separation should be usually less than 3 Å. Structures of bis-μ-chloro Ru(II) dimers reported so far are described below.

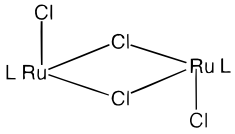

Such a structure motif happens to complexes having facial tridentate, bidentate, or monodentate ligands as reported. In our case reported here, a tripodal tetradentate TPA ligand raised a new version of bis-μ-chloro dinuclear Ru(II) structure.

To ensure the existence of the dinuclear core in solution, FAB-MS spectroscopy was used; a mixture of **3** and **4** (2.4 mM for each) in CH$_3$CN was stirred in CH$_3$CN for 24 h to show peaks due to [**3**-ClO$_4$]$^+$, [**4**-ClO$_4$]$^+$, [**3**-2(ClO$_4$)]$^+$, and [**4**-2(ClO$_4$)]$^+$ but not for scrambled species such as [(TPA)Ru(μ-Cl)$_2$Ru(5-Me$_3$-TPA)]$^{2+}$. This indicates that bis-μ-chloro Ru(II) dimers of TPA derivatives are stabilized and that the structure is maintained in CH$_3$CN solution. This is consistent with the fact that these two dimers exhibit two reversible redox waves in CV measurements in CH$_3$CN.

(32) (a) Evans, I. P.; Spencer, A.; Wilkinson, G. *J. Chem. Soc., Dalton Trans.* **1973**, 204−209. (b) Carmichael, D.; Le Floch, P.; Ricard, L.; Mathey, F. *Inorg. Chim. Acta* **1992**, *198*−*200*, 437−441.
(33) Henn, M.; Alessio, E.; Mestroni, G.; Calligaris, M.; Attia, W. M. *Inorg. Chim. Acta* **1991**, *187*, 39−50.
(34) Kojima, T.; Tsuchiya, J.; Nakashima, S.; Ohya-Nishiguchi, H.; Yano, S.; Hidai, M. *Inorg. Chem.* **1992**, *31*, 2333−2340.

Table 8. Coordination Shifts in ^{1}H NMR Spectra for **1**−**4** Relative to Corresponding Free Ligands in CD_3CN[a]

	CH_2	pyr-H3	pyr-H4	pyr-H5	pyr-H6	Me
1	0.895 (ax)	−0.613 (ax)	−0.192 (ax)	−0.003 (ax)	1.353 (ax)	0.870 (DMSO)[b]
	0.995, 1.973 (eq)	−0.094 (eq)	0.056 (eq)	0.068 (eq)	0.248 (eq)	
3	0.459 (ax)	−0.755 (ax)	−0.372 (ax)	−0.208 (ax)	0.335 (ax)	
	0.768, 1.319 (eq)	−0.139 (eq)	−0.025 (eq)	−0.306 (eq)	−0.053 (eq)	
2	0.718 (ax)	*c*	*c*		1.228 (ax)	0.032 (ax)
	0.883, 1.625 (eq)				0.270 (eq)	−0.038 (eq)
						0.294 (DMSO)[b]
4	0.513 (ax)	*c*	*c*		0.320 (ax)	−0.174 (ax, s)
	0.774, 1.391 (eq)				−0.036 (eq)	−0.386 (eq, s)

[a] Coordination shift = δ(complex) − δ(ligand). Positive value indicates a downfield shift and negative one represents an upfield shift. [b] A singlet for methyl group of free DMSO was observed at 2.549 ppm in CD_3CN. [c] Not available because signals due to those hydrogens of free 5-Me_3-TPA were observed as ill-resolved multiplets. See text.

As shown in Table 7, the structure of Ru(III) monomeric complex **5** showed longer bond distances for Ru−N(py) bonds and Ru−N(amine) than those of Ru(II) dimeric complex **3**, in contrast, Ru−Cl bond lengths are shorter in **5** than in **3**. The shorter bond lengths of Ru^{III}−Cl bonds are ascribed to stronger Coulomb interaction due to increase of positive charge of the Ru center. Fewer dπ electrons at the Ru center results in the reduction of π-back-bonding and the longer bond lengths of Ru−N(py)'s. This tendency has been observed in the Ru(II) and Ru(III) complexes with bpy,[26] isonicotinamide,[35] and pyrazine.[36] The shorter bond length of Ru^{II}−N(amine) than that of Ru^{III}−N(amine) is indicative of the fact that the strong π-acceptor character of pyridine moieties reduces electron density at the Ru(II) center, and this causes strengthened σ-donation of the tertiary amino group. In the related complex **7** reported by Che and co-workers, bond distances of Ru^{III}−N(py) are in the range of 2.083(5)−2.101(5) Å and that of Ru^{III}−N(*tert*-amine) is 2.087(5) Å;[17] those are all longer than those observed in **5**. This is due to the ligation of alkoxo ligand as a strong electron donor in **7** to increase electron density at the Ru(III) center to cause electronic repulsion against binding of other moieties.

In the CV measurement of **1**, two redox couples were observed at 0.61 and 0.04 V. A variable scan-speed sweep showed that the redox couple at 0.61 V became irreversible at lower scan speed (10 mV/s) to lose the reduction wave and to show reduction wave at 0.01 V; at higher scan speed (10 V/s) no reduction wave at 0.01 V was observed and the original redox wave due to **1** was increased in intensity. This observation suggests that an EC process takes place, and we propose the isomerization between S-bound and O-bound DMSO species. Alessio and co-workers reported that CO coordination to *trans*-$[Ru^{III}Cl_4(DMSO)_2]^-$ afforded *trans*-$[Ru^{III}Cl_4(DMSO)(CO)]^-$ in which one of two trans S-bound DMSO ligands was replaced while the other underwent linkage isomerization due to the competition for π-electrons.[37] In our case, the pyridine moiety of the TPA which is trans to the S-bound DMSO exerts similar effects to induce the isomerization in the course of CV measurements. In sharp contrast, the CV of **2** gave only one clearly reversible redox couple at 0.52 V. The lower redox potential relative to that of **1** and the lack of any EC process for **2** indicate the increased electron density at the Ru center and the strengthened Ru−S bond due to increasing π-back-bonding from the Ru center to the S═O moiety in **2**.

The ^{1}H NMR spectra of **1**−**4** allow us to access to understanding σ-donation and π-back-donation among Ru(II) centers and ligands. For this purpose, coordination shifts ($\Delta\delta$ = δ(complex) − δ(free ligand)) of **1**−**4** in CD_3CN are listed in Table 8. As for the methylene hydrogens, all are downfield-shifted to indicate the tertiary amino group coordinates as a σ-donor. Compared with the axial methylene hydrogens, equatorial ones showed larger downfield shifts, suggesting that the equatorial pyridine rings are more electron deficient than the axial pyridine because the axial pyridine has a electron donor at the trans position in any case (such as Cl^- or DMSO) to increase its electron density. Note that the DMSO ligand acts as a σ-donor as we observe downfield shift of the signal due to the methyl hydrogens; however, DMSO undergoes π-back-bonding. As indicated by EHMO calculations, HOMO is one of dπ orbitals of Ru(II) and LUMO is always π* orbitals of pyridyl moieties, and, therefore, this suggests that the pyridyl group is the strongest π-acceptor in the series of complexes described here.

As for the π-back-bonding from the Ru center to pyridines, the facility would be reflected on the energy gap between dπ of Ru center and pπ* of pyridine fragments. To evaluate the gap, we shed some light on MLCT bands. Changing TPA to 5-Me_3-TPA causes negative shifts in CV measurements, indicating that HOMO levels are raised by presumably more electron-donating 5-Me_3-TPA through σ-bonding. MLCT bands show no drastic changes with the change of the ligand from TPA to 5-Me_3-TPA (see Experimental Section) and coordination shifts listed in Table 8 also exhibit no significant alteration. These observations suggest that Ru-dπ and py-pπ* are cooperatively linked together to undergo electron donation and π-back-donation.

Conclusion

We have described here the synthesis and characterization of Ru(II) monomers, bis-μ-chloro Ru(II) dimers, and Ru(III) monomers having tripodal tetradentate TPA and 5-Me_3-TPA as ligands. The synthesis was well controlled to obtain those complexes in the appropriate oxidation states and achieved moderate to high yields as main products by changing reaction conditions. The synthetic procedures described in this paper will contribute to versatile synthesis of ruthenium compounds having TPA and related ligands. Three representative molecular structures were unambiguously established by X-ray crystallography. The structures indicate that TPA derivatives bind to both Ru(II) and Ru(III) center as tetradentate ligands; however, steric constraint causes the distortion of the Ru coordination sphere, the strong π-back-bonding interaction from the Ru center to pyridyl moieties holds the tetradentate configuration and contributes to the stability of the complexes. The π-back-

(35) Richardson, D. E.; Walker, D. D.; Sutton, J. E.; Hodgson, K. O.; Taube, H. *Inorg. Chem.* **1979**, *18*, 2216−2221.
(36) Gress, M. E.; Creutz, C. Quicksall, C. L. *Inorg. Chem.* **1981**, *20*, 1522−1528.
(37) Alessio, E.; Bolle, M.; Milani, B.; Mestroni, G.; Faleschini, P.; Geremia, S.; Calligaris, M. *Inorg. Chem.* **1995**, *34*, 4716−4721.

bonding interaction and the σ-bonding interaction between Ru centers and pyridine moieties are cooperative, and this is an essential aspect to consider properties and reactivity of Ru−(TPA derivatives) complexes.

Acknowledgment. This work was supported by Grants-in-Aid for Encouragement of Young Scientists (08740523 and 09740495 for T.K.) from The Ministry of Education, Science, and Culture of Japan. T.K. also appreciates partial support from Nissan Science Foundation and Professor Yoshihito Watanabe (Institute for Molecular Science, Okazaki, Japan) for his generous support. We thank Ms. Mie Tomonou for her expertise to obtain FAB-MS data and Ms. Kaori Nakamura for her help in CV measurements.

Supporting Information Available: Tables of complete data collection information, bond distances, bond angles, positional parameters, and anisotropic thermal factors for **2**, **3**, and **5** (33 pages). Ordering information is given on any current masthead page.

IC971049H